

# Geophysical Research Letters<sup>®</sup>



## RESEARCH LETTER

10.1029/2023GL103864

### Key Points:

- We observed intracloud negative dart-stepped leaders producing regular trains of broadband electromagnetic microsecond-scale pulses
- Very High Frequency sources follow channels of previous leaders occurring within the same flash tens of milliseconds before the reported observations
- Conductivity of decaying channels and strength of the ambient electric field might act together to trigger this unusual stepping process

### Supporting Information:

Supporting Information may be found in the online version of this article.

### Correspondence to:

I. Kolmašová,  
iko@ufa.cas.cz

### Citation:

Kolmašová, I., Scholten, O., Santolík, O., Hare, B. M., Zacharov, P., Lán, R., et al. (2023). A strong pulsing nature of negative intracloud dart leaders accompanied by regular trains of microsecond-scale pulses. *Geophysical Research Letters*, 50, e2023GL103864. <https://doi.org/10.1029/2023GL103864>

Received 26 MAR 2023

Accepted 6 MAY 2023

### Author Contributions:

**Conceptualization:** I. Kolmašová

**Data curation:** R. Lán

**Formal analysis:** I. Kolmašová, O.

Scholten, P. Zacharov

**Methodology:** I. Kolmašová, O. Scholten

**Validation:** O. Santolík




**Writing – original draft:** I. Kolmašová,

O. Scholten, P. Zacharov

**Writing – review & editing:** O. Santolík,

B. M. Hare, N. Liu, J. R. Dwyer

## A Strong Pulsing Nature of Negative Intracloud Dart Leaders Accompanied by Regular Trains of Microsecond-Scale Pulses

I. Kolmašová<sup>1,2</sup> , O. Scholten<sup>3</sup> , O. Santolík<sup>1,2</sup> , B. M. Hare<sup>4</sup> , P. Zacharov<sup>5</sup>, R. Lán<sup>1</sup>, N. Liu<sup>6</sup> , and J. R. Dwyer<sup>6</sup> 

<sup>1</sup>Department of Space Physics, Institute of Atmospheric Physics of the Czech Academy of Sciences, Prague, Czechia,

<sup>2</sup>Faculty of Mathematics and Physics, Charles University, Prague, Czechia, <sup>3</sup>University Groningen, Kapteyn Astronomical Institute, Groningen, The Netherlands, <sup>4</sup>ASTRON, Dwingeloo, The Netherlands, <sup>5</sup>Department of Meteorology, Institute of Atmospheric Physics of the Czech Academy of Sciences, Prague, Czechia, <sup>6</sup>Department of Physics and Astronomy, Space Science Center (EOS), University of New Hampshire, Durham, NH, USA

**Abstract** We report the first observations of negative intracloud (IC) dart-stepped leaders accompanied by regular trains of microsecond-scale pulses, simultaneously detected by shielded broadband magnetic loop antennas and the radio telescope Low Frequency Array (LOFAR). Four investigated pulse trains occurred during complicated IC flashes on 18 June 2021, when heavy thunderstorms hit the Netherlands. The pulses within the trains are unipolar, a few microseconds wide, and with an average inter-pulse interval of 5–7  $\mu$ s. The broadband pulses perfectly match energetic, regularly distributed, and relatively isolated bursts of very high frequency sources localized by LOFAR. All trains were generated by negative dart-stepped leaders propagating at a lower speed than usual dart leaders. They followed channels of previous leaders occurring within the same flash several tens of milliseconds before the reported observations. The physical mechanism remains unclear as to why we observe dart-stepped leaders, which show mostly regular stepping, emitting energetic microsecond-scale pulses.

**Plain Language Summary** Lightning phenomena inside thunderclouds can be explored using their electromagnetic radiation. To study these processes at small temporal and spatial scales, we combine broadband magnetic loop antennas with the Low Frequency Array (LOFAR) radio telescope. Measurements of broadband antennas acquired during a severe Dutch thunderstorm showed pulse sequences composed of tens microsecond-scale unipolar pulses, which were surprisingly regularly distributed. Such regular pulse trains have been rarely reported from previous observations. When we thoroughly lined up the timestamps of both simultaneously measuring observational systems, we found that the regular broadband pulses perfectly match with localized isolated bursts of energetic very high frequency radiation detected by LOFAR. The 3D mapping of the radio sources of these bursts allowed us to place the investigated events into the context of the parent intracloud (IC) lightning flash. The results revealed negative IC dart leaders, which propagated along the preconditioned channels originally formed by previous positive or negative IC leaders. Some of these dart leaders then exhibited unusual stepping manifested by the observed regular pulses. We assume that a favorable combination of the conductivity of preexisting lightning channels and the strength of the ambient electric field inside thunderclouds might be needed to trigger this unusual stepping.

## 1. Introduction

Lightning processes often occur in repeating patterns with rates ranging from units of microseconds to fractions of a second. Among these processes, the most explored ones are parts of lightning flashes, which take place below the thundercloud, as the Return Strokes (RSs), stepped leaders, dart leaders, dart-stepped leaders, and M-components in cloud-to-ground (CG) discharges, which have been investigated for many decades. Both optical and electromagnetic records confirm that individual lightning strokes within multi-stroke flashes are typically separated by several tens of milliseconds (Poelman et al., 2021). The repetition rate of stepped leader pulses is about several tens of kHz (Lu et al., 2008) and the dart-stepped leader pulses occur in a succession, which is as short as several microseconds (Jiang et al., 2014). The incloud processes, as lightning initiation or propagation of intracloud (IC) leaders, are usually not visible for high-speed cameras. When exploring them, we have to rely on electromagnetic measurements. Sequences of initial (or preliminary) breakdown (IB) pulses are believed to accompany the initiation of majority of CG and IC discharges in their electromagnetic records (Marshall

© 2023. The Authors.

This is an open access article under the terms of the [Creative Commons Attribution License](#), which permits use, distribution and reproduction in any medium, provided the original work is properly cited.

et al., 2014). The IB pulses are bipolar, separated by several tens to a few hundreds of microseconds in CG flashes and by several hundreds of microseconds in normal IC flashes (Kolmašová et al., 2019; Marshall et al., 2013; Scholten, Hare, Dwyer, Liu, Sterpka, Kolmašová, et al., 2021; Smith et al., 2018; Yang et al., 2023).

After the initiation of a flash, positive and negative leaders propagate through the thundercloud forming hot and conductive plasma channels. Positive and negative leaders behave differently. The space stem mechanism of extension of negative leaders causes their stepping manifested by the presence of pulses in the electromagnetic records. The channels of positive leaders develop more continuously and thus are poorly detectable in electromagnetic recordings (Visacro et al., 2017). Nevertheless, recent observations provided evidence of stepping also during the prolongation of positive leaders (Jiang et al., 2020).

Sometimes new leaders retrace the channels previously established by slower leaders propagating in a virgin air. These leaders can travel a significant distance through both former positive and negative leader channels. The terminology used for leaders following the previously established plasma channel is unfortunately somewhat inconsistent. The leaders occurring within CG flashes below the cloud base are called dart or dart-stepped leaders (Biagi et al., 2010; Dwyer & Uman, 2014; Petersen & Beasley, 2013; Stolzenburg et al., 2019; D. Wang et al., 2016; J. Wang et al., 2022). Leaders, which do not reach the ground and stay inside the thundercloud, were named K-leaders, recoil leaders, and also dart leaders (Jensen et al., 2021). Ogawa and Brook (1964) originally defined negative recoil leaders as leaders traveling along the preceding positive leader channels toward their origin. This behavior was confirmed by optical observations (Saba et al., 2008). Mazur et al. (2013) suggested using a term “dart leader” only for recoil leaders, which reach the ground. Jensen et al. (2021) tried to consolidate the terminology suggesting to use “dart leader” as a general term for all leaders (both retrograde leaders on positive channels and prograde leaders on negative channels), which travel in already ionized channels at a higher speed than previous leaders propagating in a virgin air. As not all the leaders investigated in our study fit the original definition of recoil leaders by Ogawa and Brook (1964), we will follow Jensen et al. (2021) and use a term “dart leader” to describe our observations.

One of the poorly understood in-cloud phenomena are the trains of regularly distributed unipolar microsecond-scale pulses, which occur in electromagnetic measurements conducted during the evolution of both CG and IC flashes. These trains were for the first time described by Krider et al. (1975), who suggested that observed pulse trains could be produced by K-changes developing in a stepped manner. Rakov et al. (1992) found that only 24% of observed K-changes were accompanied by microsecond-scale pulses. Davis (1999), Krider et al. (1975), and Y. Wang et al. (2021) found that duration of an average interpulse interval in regular pulse trains occurring within IC flashes was about 5  $\mu$ s. The pulse repetition rates and peak pulse amplitudes tend to decrease toward the end of the train (Kolmašová & Santolík, 2013; Rakov et al., 1992, 1996). Rakov et al. (1996) noted rare reversals of the polarity of pulses within several observed trains and attributed this effect to the changes of the channel geometry. Based on the evolution of pulse spacing and pulse polarity changes Y. Wang et al. (2010) divided the regular pulse trains into four categories (normal, back, symmetry, and reversal trains) and showed a temporal correspondence of pulses observed by a broadband (0–10 MHz) instrument and power peaks detected by a Very High Frequency (VHF) receiver (267–273 MHz). Zhu et al. (2014) investigated a convective storm in Shanghai, and found that over 98% of observed K changes (from more than one thousand cases) were associated with a microsecond-scale pulse activity. The pulses were grouped in regular trains only in 9% of events. Y. Wang et al. (2021) found that the leaders generating regular pulse trains occurred usually in the middle of an IC flash, and propagated at a velocity of  $1.2\text{--}3 \times 10^6$  m/s, slower than both the dart leaders or dart-stepped leaders in CG flashes. Using an array of 12 electric field antennas, Shi et al. (2020) found that a majority of pulse trains propagated through the main negative charge region. Jiang et al. (2022) combined optical images and mapping of VHF radiation sources, and hypothesized that long dart leaders (referred to as recoil leaders in that work) activated negative breakdown at the opposite end of a corresponding channel network at the time when the regular pulse trains were observed.

Using the radio telescope Low Frequency Array (LOFAR), Hare et al. (2023) recently showed that the propagation speed of five investigated dart leaders (again referred to as recoil leaders in that paper) varied from  $5 \times 10^6$  to  $2.5 \times 10^7$  m/s, the intensity of the emitted VHF radiation usually decreased when the leader speed slowed down, and that the dart leaders had meter-scale tortuosity but without any evidence of stepping.

In the present study, we for the first time combine broadband magnetic field measurements with the data provided by LOFAR during the observational campaign conducted in summer 2021, in order to bring new information about regular microsecond-scale pulse trains and provide new constraints to future modeling of incloud

dart-stepped leaders. In Section 2, we introduce our instrumentation and data set. In Section 3, we describe our observations. In Sections 4 and 5, we discuss and summarize our findings.

## 2. Instrumentation and Data Set

### 2.1. Broadband Magnetic Loop Antenna

To obtain the time derivative of variations of the magnetic field in the frequency range from 5 kHz up to 90 MHz we use two perpendicular Shielded Loop Antenna with a Versatile Integrated Amplifier (SLAVIA) sensors, which provide us with broadband measurements of two horizontal magnetic field components (Kolmašová et al., 2018, 2022; Scholten, Hare, Dwyer, Sterpka, et al., 2021; Scholten et al., 2022). The antenna signals are sampled at a frequency of 200 MHz by a digital oscilloscope. The digitized signal is numerically integrated. The sensitivity of the system is  $6 \text{ nT/s}/\sqrt{\text{Hz}}$  which corresponds to  $1 \text{ fT}/\sqrt{\text{Hz}}$  at 1 MHz. The system works in a triggered mode: it records a 168-ms long waveform snapshot including a history of 52 ms when receiving a trigger. The trigger is time tagged by the Global Positioning System receiver with an accuracy of  $1 \mu\text{s}$ . The antennas have been installed close to Ter Wisch, the Netherlands, at a site located 15.1 km to the East and 0.6 km to the North with respect to the LOFAR core. The azimuth of the SLAVIA 1 antenna is  $150^\circ$ ; the loop of SLAVIA 2 is oriented at an azimuth of  $66^\circ$ . Positive downward current pulse at an azimuth of  $150^\circ$  from the position of SLAVIA 1 (and within an interval of  $\pm 90^\circ$  around this direction) causes an initial positive polarity of a measured magnetic field pulse. SLAVIA 2 gives the same response for a positive downward current at an azimuth of  $66^\circ$  from its position.

### 2.2. Low Frequency Array (LOFAR)

LOFAR is a radio telescope consisting of several thousand antennas spread over much of Europe that is primarily build for astronomical observations. For the present observations we record the signals of selected antennas in Dutch stations only, amounting to about 170 dual-polarized antennas spread over 34 stations, operating in the 30–80 MHz VHF-band with base lines up to 100 km.

### 2.3. Data Set

The data set used in this study was recorded during an observational campaign in summer 2021, when broadband magnetic field measurements were synchronized with LOFAR. On 18 June 2021, the Netherlands was hit by strong convective storms, which brought large hail (up to 5 cm), severe wind and also local flooding, as result of a frontal boundary in a large trough located near the coastline of the Western Europe (detailed information about the meteorological context of our observations is given in Text S1 and Figure S1 in Supporting Information S1).

During this day, nine overlapping records of the broadband magnetic antenna and LOFAR were acquired. Integrated magnetic field waveforms were searched for a presence of regular microsecond-scale pulse trains. Nine trains were found in three 168 ms long broadband recordings, starting at 17:46:58.278 (event C1—1 train), 18:58:48.255 (event C5—5 trains), and 20:11:51.821 (event C9—3 trains). The corresponding LOFAR recordings (of typically 1.5 s) start at 17:46:57 (C1), 18:58:47 (C5), and 20:11:50 (C9). For our analysis we selected four trains (marked in following text C1, C5, C9-1, and C9-2), which were composed of more than 10 pulses, and which were well recognizable in records of the two perpendicular broadband antennas. We have then chosen the antenna in which the waveform was less affected by interferences and the pulses exhibited larger peak amplitudes (SLAVIA 2 for event C1, SLAVIA 1 for other events).

To image the observations, we use two different procedures. One is called the impulsive imager, described in Scholten, Hare, Dwyer, Sterpka, et al. (2021), where a time-of-arrival-difference method is used. Arrival time differences of the pulses from a single source in different antennas are calculated using interferometric cross correlations. In the other imaging method, called TRI-D (Scholten, Hare, Dwyer, Liu, Sterpka, Buitink, et al., 2021; Scholten et al., 2022), the image space is voxelated where for each voxel the beam-formed time trace is calculated. For each 100-ns section of the time trace, the voxel with the maximum intensity is taken as the source location. For beamforming a coherent sum over all antenna traces is made while keeping track of their polarization.

## 3. Observations

As the first step, we analyzed the properties of magnetic field pulse trains. The pulses in the trains were unipolar, regularly distributed, with a pulse width of about 1 microsecond. Similarly, as in Kolmašová and Santolík (2013),

each individual pulse was considered to be unipolar, if the immediately following overshoot of the opposite polarity does not exceed one half of the peak amplitude of the original pulse. The magnetic field waveforms are plotted in Figure 1a (event C1), Figure 2a (event C9-1), in Figure S2a in Supporting Information S1 (event C5), and Figure S3a in Supporting Information S1 (event C9-2). Duration of the trains varied from 91 to 277  $\mu$ s. There were 19 pulses in the shortest train and 96 pulses in the longest one. The median interpulse interval varied from 4 to 7  $\mu$ s. The interpulse interval was increasing toward the end of trains C5, C9-1, and C9-2. During event C1, we observed both trends, the interpulse spacing was increasing during the first half of the train and then decreasing up to the end of the train. The results are summarized in Table 1. Based on the criteria of Y. Wang et al. (2010) trains C5, C9-1, and C9-2 can be classified as regular trains, while train C1 was a symmetric train. The peak amplitude of pulses decreased toward the end of train C1. There was no clear evolution of the pulse peak amplitude within the other three trains.

Using the LOFAR impulsive imager, we were able to estimate location of the leaders, which generated observed regular trains of magnetic field pulses. We chose the LOFAR stations closest to the emitting sources (CS002 for event C1; CS003 for event C5; RS508 for events C9-1 and C9-2), and we thoroughly corrected the timing of the LOFAR data recorded at these stations for the propagation delay. We similarly corrected the timing of the corresponding broadband magnetic field waveforms. We found that the magnetic field pulses plotted in panel (a) (Figures 1 and 2; Figures S2 and S3 in Supporting Information S1) perfectly line up with the VHF power peaks plotted in panel (b) in the same figures. This correspondence is more clearly visible in details indicated in panel (a) by a blue rectangle and plotted in panel (f). The average propagation velocity of the leaders was calculated from the moving mean position of sources along a track (see Scholten, Hare, Dwyer, Liu, Sterpka, Kolmašová, et al., 2021) and plotted in panel (c). For all events, the velocity was on the order of  $10^6$  m/s and decreased toward the end of the trains. Note that this average velocity is being calculated over groups of steps and that the formation of individual steps might be faster. The sources of VHF radiation localized by the LOFAR impulsive imager and color coded by their time of occurrence are displayed in panel (d). The leader was propagating down from 8.7 to 7.5 km during event C1 (Figure 1d), traveling up from 6.1 to 6.4 km during the short event C5 (Figure S2d in Supporting Information S1), and up from 6.5 to 6.9 km during event C9-1 (Figure 2d), and traveling down from 6 to 5.5 km during event C9-2 (Figure S3d in Supporting Information S1). Based on the impulsive imager data we estimated the length of individual leader steps to be of the order of a few tens of meters. When using the new LOFAR TRI-D imaging procedure, which includes both strong and weaker VHF sources, each broadband pulse was clearly accompanied by an isolated burst of VHF radiation sources as it is illustrated in panel (f) in Figures 1 and 2; Figures S2 and S3 in Supporting Information S1. The spread of sources for each broadband pulse has a width in space around 100 m, which is due to a combination of physical source spread and LOFAR imaging inaccuracies. Unfortunately, it is difficult to separate the two effects, since LOFAR's imaging accuracy depends highly on pulse sub-structure (Scholten et al., 2022).

By combining the location of the leaders, direction of their motion, and the relative orientation of antennas to the leader position with the polarity and relative amplitude of magnetic field pulses in both broadband antennas, we obtain a very consistent picture corresponding to negative leaders (with negative current in the direction of their motion) in all investigated cases.

To interpret our observations, we also looked at the placement of the other detected stepping leaders within the flashes imaged by the LOFAR impulsive imager. The overview plots are provided in Figures S4–S7 in Supporting Information S1, for events C1, C5, C9-1, and C9-2 respectively. The gray scale is used for the evolution of flashes outside the pulse trains episodes, which, in turn, are plotted on a color scale. The time intervals displayed by both scales are shown at the bottom of the figures. It is clear, that all imaged events can be characterized as complex and extensive IC flashes, and the stepping leaders occurred well inside their time interval, close to the boundary between the in-cloud negative and upper positive charge regions. Detailed images shown in panel (e) in Figures 1 and 2; Figures S2 and S3 in Supporting Information S1 reveal that all leaders exhibiting the microsecond scale stepping were dart-stepped leaders following the previous path of positive (events C1, C5, and C9-1) or negative leaders (event C9-2) with a delay of 13–81 ms after them, while the total duration of their parent flashes was 0.25, 0.3, and 0.4 s, respectively, as indicated in Table 1.



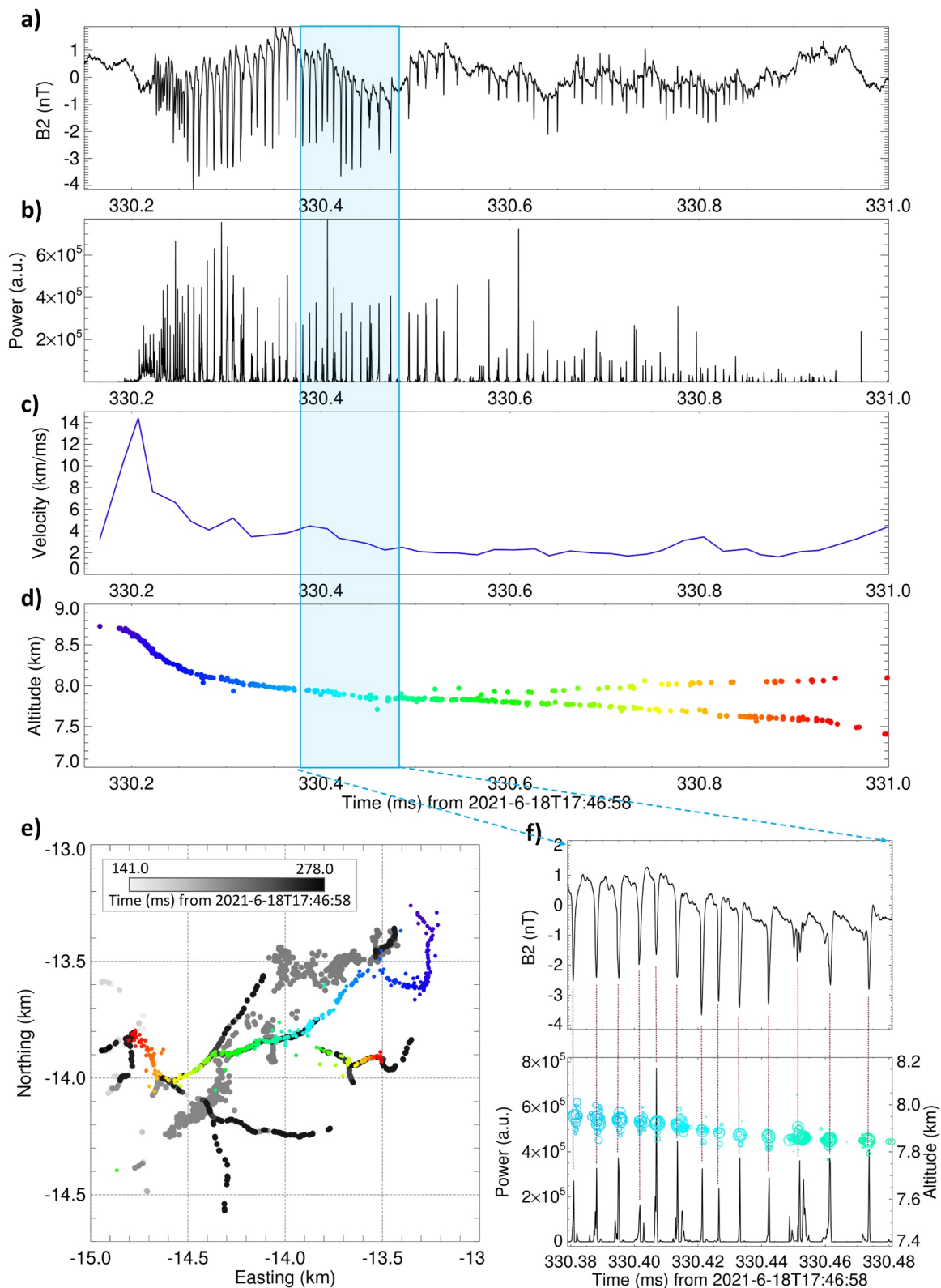


**Figure 1.** Event C1: (a) Magnetic field pulse train measured by the Shielded Loop Antenna with a Versatile Integrated Amplifier 2 antenna on 18 June 2021. (b) Very High Frequency (VHF) power detected at the same time by the Low Frequency Array (LOFAR) antenna CS002. (c) Average velocity of the leader movement. (d) Sources of VHF radiation located by the LOFAR impulsive imager. (e) A map showing a development of the flash before the pulse train was observed (in gray scale) and the leader propagation during the pulse train (color scale). (f) Detail of the magnetic field waveform together with VHF power peaks and VHF sources imaged by the LOFAR TRI-D imager. The detail is marked in panel (a) by a blue rectangle.

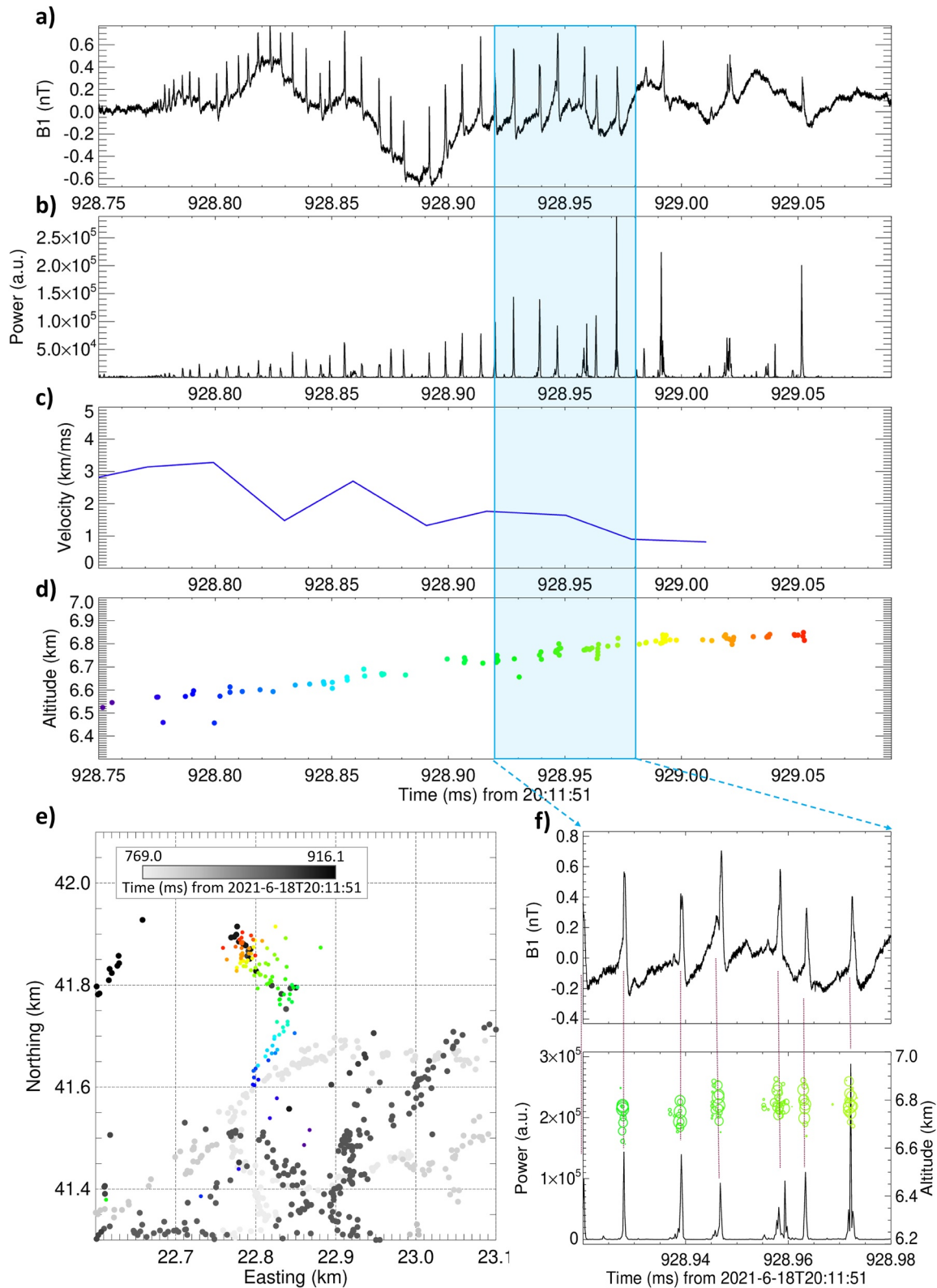


**Figure 2.** The same as in Figure 1 but for Event C9-1, in which the magnetic field waveform (a) was recorded by Shielded Loop Antenna with a Versatile Integrated Amplifier 1. The Very High Frequency power (b) was detected by the Low Frequency Array antenna RS508.

**Table 1**  
*Properties of Pulse Trains*

Train	Flash duration (s)	Train duration ( $\mu$ s)	Number of pulses	Mean interpulse interval and the standard deviation ( $\mu$ s)	Median interpulse interval ( $\mu$ s)	Interpulse spacing evolution ( $\mu$ s/100 $\mu$ s)	Time from the previous leader propagating along the same path (ms)
C1	0.25	714	96	$7.5 \pm 3.6$	7.0	+2.1 up to the half of the train, then $-2.3$	52
C5	0.3	91	19	$5.1 \pm 3.2$	4.0	+6.7	81
C9-1	0.4	277	41	$6.9 \pm 5.3$	6.0	+4.3	13
C9-2	0.4	273	54	$5.2 \pm 4.7$	4.0	+3.9	54

#### 4. Discussion

Owing to the limited duration of the broadband magnetic field records (168 ms), which covered only about 40%–60% of the three investigated IC flashes observed by LOFAR on 18 July 2021, we were unable to inspect all dart leaders occurring within these flashes for the presence of regular microsecond-scale pulse trains. However, the collected data allowed us to concentrate on a detailed analysis of several recorded sequences. The four investigated pulse trains possess the same temporal properties as previously reported sequences of microsecond-scale pulses measured in various geographical and meteorological conditions (Kolmašová & Santolík, 2013; Krider et al., 1975; Rakov et al., 1992, 1996; Y. Wang et al., 2010; Zhu et al., 2014). It indicates that the fundamental process, which triggers the observed regular pulse bursts, might be the same as in all other published events. Because of the lower frequency limit of our instrumentation at 5 kHz, we were unable to verify the presence of slow K-changes accompanying the analyzed pulse trains.

The pulses within the trains investigated in our case study were not extremely strong, only those, which occurred during event C1 had peak amplitudes comparable to peak amplitudes of typical IB pulses (a few tens of percent of the corresponding (RS amplitudes) normalized to similar distance from the source discharge (Kolmašová et al., 2018)). In other three cases the pulse amplitudes were similarly strong as the stepped leader pulses in CG flashes. It is thus possible that the processes generating the regular pulse trains occur more frequently, but the pulses might be too small to be recognizable in electromagnetic recording at larger distances. As regards the power of the VHF sources, these were, in all observed events, by one to two orders of magnitude stronger than intensely radiating negative leaders (IRNL) reported by Scholten, Hare, Dwyer, Liu, Sterpka, Kolmašová, et al. (2021).

We discovered that all stepping leaders generating regular pulse trains were negative dart-stepped leaders (in agreement with Shi et al., 2020) following pre-existing plasma channels after several tens of milliseconds (C1: 52 ms; C5: 81 ms; C1-9: 13 ms, and C9-2: 54 ms). Estimation of these delays is based on the location of the previously occurring sources imaged by the LOFAR impulsive imager. We cannot rule out that these delays were shorter because of poorly imaged parts of the path of preceding positive leaders. Most delays between the dart leaders and their predecessors reported by Hare et al. (2023) ranged from 15 to 32 ms, and were thus comparable to our observations with one exception of a very long delay of 170 ms in their records. The dart-stepped leaders described in our study propagated at a slightly smaller speed than usual dart leaders reported by Hare et al. (2023). The leader propagation speed was decreasing within the trains while the propagation steps approximately kept their spatial scale during the time intervals manifested by the presence of regular pulse trains. This was reflected by increasing interpulse time intervals, similarly as in the studies by Kolmašová and Santolík (2013) or Rakov et al. (1996).

We do not see any correlation between the pulse peak amplitudes and power of corresponding VHF pulses. Kolmašová et al. (2019) also reported the lack of correlation between amplitudes of broadband IB pulses and the peak power of the corresponding VHF pulses. It implies that the strength of streamers occurring at the beginning of the step formation (reflected in the power of sources imaged by LOFAR) does not correlate with the magnitude of currents flowing in these steps (measured by the magnetic loops).

There are nearly no other reports describing properties of dart-stepped leaders in IC flashes, then those reporting similar pulse trains (Rakov et al., 1996; Shi et al., 2020; Y. Wang et al., 2010; Zhu et al., 2014). As concerns comparison with dart-stepped leaders in natural or triggered CG lightning, Stolzenburg et al. (2019) investigated

a transition between the dart leader and subsequent stepped leader preceding subsequent lightning strokes in negative CG flashes. Just a millisecond before the transition from the dart leader traveling in an existing path to the stepped leader forming a new path, a train of relatively intense unipolar pulses similar to our observation occurred in the displayed electric field records (their Figure 12b). This indicates that changes in the conditioning of the existing channels control the stepping and that the time delay between the observed dart-stepped leaders and the preceding leaders does not seem to be the only parameter controlling the initiation of the stepping process. The dart-stepped leaders in triggered CG lightning in the study by Wang et al. occurred 25, 50, and 127 ms after the preceding stroke, in a similar broad range of values as found by Hare et al. (2023), and as we also obtained in the present study.

In a study of rocket and wire triggered flashes, the dart-stepped leader propagated downward at an average speed between  $2.7 \times 10^6$  and  $3.4 \times 10^6$  m s<sup>-1</sup> (Biagi et al., 2010), very close to the propagation speeds of incloud dart-stepped leaders observed in our study. The propagation velocity of dart-stepped leaders fluctuated without any clear trend in the study of J. Wang et al. (2022), in contrast with the deceleration of the dart-stepped leader velocities in our study. The pulses generated by CG dart-stepped leaders were not regularly distributed in measurements of the time derivative of electric field in Dwyer and Uman (2014, their Figure 4.10) and the larger ones were found to be accompanied by X-ray bursts. Such observation was not reported for regular pulse trains in IC dart-stepped leader up to now.

Finally, measurements of microwaves at 1.57 GHz radiated by a dart-stepped leader in natural CG flashes, as reported by Petersen and Beasley (2013), showed power peaks approximately every 5 μs, the pulses were quite regularly spaced and interpulse noise was much lower than in case of regular step leaders. The authors explain the interpulse noise in step leaders by a presence a corona streamer zone which might have been absent in case of dart-stepped leaders. This is exactly what we can see in our case study: isolated VHF power bursts lined up with broadband pulses, separated by about 5 μs with no or very weak VHF activity between pulses.

## 5. Conclusions

Our new observations of relatively rarely occurring in-cloud negative dart-stepped leaders accompanied by regular pulse trains lead to the following results:

- (a) Delays of several tens of milliseconds after the previous leaders traveling in the same channel falls in a similar range as it was previously observed for non-stepping dart leaders (Hare et al., 2023) or in the dart-stepped leaders in triggered CG lightning (J. Wang et al., 2022).
- (b) The leaders generate the electromagnetic microsecond-scale pulse trains lasting several hundred of microseconds. The trains consist of regularly distributed unipolar pulses spaced by about 5 μs.
- (c) Each leader step generates a relatively weak broadband pulse accompanied by an isolated burst of intense VHF radiation with very high peak power, which was 10 times more powerful than individual power peaks in intensely radiating negative leaders (IRNL). These isolated power peaks were separated by VHF quiet periods unlike IRNLs, which radiate nearly continuously (Scholten et al., 2022).
- (d) We were able to locate the events close to the boundary between the thundercloud charge centers, where we expect high ambient electric fields.
- (e) The average propagation velocities (units of km/ms) of observed events are slower than in case of usual dart leaders, but very similar to these of dart-stepped leader, which precede the subsequent CG RSs and are observed below the cloud base. Individual leader steps are about a few tens of meters long.
- (f) In contrast with events from our study, pulses generated by dart-stepped leaders in CG flashes occur commonly in both natural and triggered CG flashes, but do not form well-defined trains with regularly distributed pulses.

These properties of observed incloud dart-stepped leaders, which emitted regular pulse trains, and a relative rareness of their observations with respect to their CG counterparts lead us to an assumption that suitable conditions for formation of dart-stepped leaders are fulfilled more often below the cloud base than inside the thundercloud. We thus hypothesize that a favorable combination of the conditioning of decaying plasma channels, their geometry on a meter scale (Hare et al., 2023), and a strength of the ambient electric field is required to trigger the stepping process manifested by regular pulse trains. We assume that the thunderstorm severity might play a significant role in the formation of these suitable conditions, as severe thunderstorms are known for very strong updrafts, which are heavily involved in distribution of hydrometeors and their electrification (Baker et al., 1999).



Indeed, the thunderstorm, which hosted the events for this case study, was extremely severe (very high CAPE of 2400 J/kg and a very large wind shear of 18 m/s) when compared with several thousands of severe European convective storms occurring during the warm seasons in 2006 and 2007 (Kaltenböck et al., 2009). Extended data set of dart-stepped leaders coming with pulse trains, as well as relevant meteorological contexts of their observations are needed to verify our hypotheses. Nevertheless, this case study can provide new constraints to future modeling of incloud dart-stepped leaders.

### Data Availability Statement

The LOFAR data are available from the LOFAR Long Term Archive ([https://www.astron.nl/lofarwiki/doku.php?id=public:lta\\_howto](https://www.astron.nl/lofarwiki/doku.php?id=public:lta_howto)). To download this data, please create an account and follow the instructions for “Staging Transient Buffer Board data.”

The broadband SLAVIA antenna data used in this study are available at <https://doi.org/10.17632/g2m644tnz3.1> (Kolmašová, 2023).

### Acknowledgments

The work of IK, OS, and RL was supported by the GACR Grant 20-09671S and by the European Regional Development Fund CREAT project (CZ.02.1.01/0.0/0.0/15\_003/0000481). BMH is funded by ERC Grant agreement 101041097. The contribution of PZ was supported by the GACR Grant 23-06430S.

### References

- Baker, M. B., Blyth, A. M., Christian, H. J., Latham, J., Miller, K. L., & Gadian, K. L. (1999). Relationships between lightning activity and various thundercloud parameters: Satellite and modelling studies. *Atmospheric Research*, 51(3–4), 221–236. [https://doi.org/10.1016/S0169-8095\(99\)00009-5](https://doi.org/10.1016/S0169-8095(99)00009-5)
- Biagi, C. J., Uman, M. A., Hill, J. D., Jordan, D. M., Rakov, V. A., & Dwyer, J. (2010). Observations of stepping mechanisms in a rocket-and-wire triggered lightning flash. *Journal of Geophysical Research*, 115(D23), D23215. <https://doi.org/10.1029/2010JD014616>
- Davis, S. M. (1999). Properties of lightning discharges from multiple-station wide band measurements. The dissertation presented to the Graduate school of the University of Florida, UMI Microform 9945961.
- Dwyer, J. R., & Uman, M. A. (2014). The physics of lightning. *Physics Reports*, 534(4), 147–241. <https://doi.org/10.1016/j.physrep.2013.09.004>
- Hare, B. M., Scholten, O., Buitink, S., Dwyer, J. R., Liu, N., Sterpka, C., & ter Veen, S. (2023). Characteristics of recoil leaders as observed by LOFAR. *Physical Review D*, 107(2), 023025. <https://doi.org/10.1103/PhysRevD.107.023025>
- Jensen, D. P., Sonnenfeld, R. G., Stanley, M. A., Edens, H. E., da Silva, C. L., & Krehbiel, P. R. (2021). Dart-leader and K-leader velocity from initiation site to termination time-resolved with 3D interferometry. *Journal of Geophysical Research: Atmospheres*, 126(9), e2020JD034309. <https://doi.org/10.1029/2020JD034309>
- Jiang, R., Qie, X., Li, Z. X., Zhang, H., Li, X., Yuan, S., et al. (2020). Luminous crown residual vs. bright space segment: Characteristic structures for the intermittent positive and negative leaders of triggered lightning. *Geophysical Research Letters*, 47(21), e2020GL088107. <https://doi.org/10.1029/2020GL088107>
- Jiang, R., Wu, Z., Qie, X., Wang, D., & Liu, M. (2014). High-speed video evidence of a dart leader with bidirectional development. *Geophysical Research Letters*, 41(14), 5246–5250. <https://doi.org/10.1002/2014GL060585>
- Jiang, R., Yuan, S., Qie, X., Liu, M., & Wang, D. (2022). Activation of abundant recoil leaders and their promotion effect on the negative-end breakdown in an intracloud lightning flash. *Geophysical Research Letters*, 49(1), e2021GL096846. <https://doi.org/10.1029/2021GL096846>
- Kaltenböck, R., Diendorfer, G., & Dotzek, N. (2009). Evaluation of thunderstorm indices from ECMWF analyses, lightning data and severe storm reports. *Atmospheric Research*, 93(1–3), 381–396. <https://doi.org/10.1016/j.atmosres.2008.11.005>
- Kolmašová, I. (2023). Magnetic loop antennas data for the manuscript “A strong pulsing nature of negative intracloud dart leaders accompanied by regular trains of microsecond-scale pulses”, Mendeley Data, V1. <https://doi.org/10.17632/g2m644tnz3.1>
- Kolmašová, I., Marshall, T., Bandara, S., Karunaratne, S., Stolzenburg, M., Karunaratne, N., & Siedlecki, R. (2019). Initial breakdown pulses accompanied by VHF pulses during negative cloud-to-ground lightning flashes. *Geophysical Research Letters*, 46(10), 5592–5600. <https://doi.org/10.1029/2019GL082488>
- Kolmašová, I., & Santolík, O. (2013). Properties of unipolar magnetic field pulse trains generated by lightning discharges. *Geophysical Research Letters*, 40(8), 1637–1641. <https://doi.org/10.1002/grl.50366>
- Kolmašová, I., Santolík, O., Defer, E., Rison, W., Coquillat, S., Pedebay, S., et al. (2018). Lightning initiation: Strong VHF radiation sources accompanying preliminary breakdown pulses during lightning initiation. *Scientific Reports*, 8(1), 3650. <https://doi.org/10.1038/s41598-018-21972-z>
- Kolmašová, I., Santolík, O., Šlegl, J., Popová, J., Sokol, Z., Zacharov, P., et al. (2022). Continental thunderstorm ground enhancement observed at an exceptionally low altitude. *Atmospheric Chemistry and Physics*, 22(12), 7959–7973. <https://doi.org/10.5194/acp-22-7959-2022>
- Krider, E. P., Radda, G. J., & Noggle, R. C. (1975). Regular radiation field pulses produced by intracloud lightning discharges. *Journal of Geophysical Research*, 80(27), 3801–3804. <https://doi.org/10.1029/jc080i027p03801>
- Lu, W., Wang, D., Takagi, N., Rakov, V., Uman, M., & Miki, M. (2008). Characteristics of the optical pulses associated with a downward branched stepped leader. *Journal of Geophysical Research*, 113(D21), D21206. <https://doi.org/10.1029/2008JD010231>
- Marshall, T., Schulz, W., Karunaratna, N., Karunaratne, S., Stolzenburg, M., Vergeiner, C., & Warner, T. (2014). On the percentage of lightning flashes that begin with initial breakdown pulses. *Journal of Geophysical Research: Atmospheres*, 119(2), 445–460. <https://doi.org/10.1002/2013JD020854>
- Marshall, T., Stolzenburg, M., Karunaratne, S., Cummer, S., Lu, G., Betz, H.-D., et al. (2013). Initial breakdown pulses in intracloud lightning flashes and their relation to terrestrial gamma ray flashes. *Journal of Geophysical Research: Atmospheres*, 118(19), 10907–10925. <https://doi.org/10.1002/jgrd.50866>
- Mazur, V., Ruhnke, L. H., Warner, T. A., & Orville, R. E. (2013). Recoil leader formation and development. *Journal of Electrostatics*, 71(4), 763–768. <https://doi.org/10.1016/j.elstat.2013.05.001>
- Ogawa, T., & Brook, M. (1964). The mechanism of the intracloud lightning discharge. *Journal of Geophysical Research*, 69(24), 5141–5150. <https://doi.org/10.1029/JZ069i024p05141>
- Petersen, D. A., & Beasley, W. H. (2013). High-speed video observations of a natural negative stepped leader and subsequent dart-stepped leader. *Journal of Geophysical Research: Atmospheres*, 118(21), 12110–12119. <https://doi.org/10.1002/2013JD019910>

- Poelman, D., Schultz, W., Pedebay, S., Campos, L. Z. S., Matsui, M., Hill, D., et al. (2021). Global ground strike point characteristics in negative downward lightning flashes—Part 1: Observations. *Natural Hazards and Earth System Sciences*, 21(6), 1921–1933. <https://doi.org/10.5194/nhess-21-1921-2021>
- Rakov, V. A., Thottappillil, R., & Uman, M. A. (1992). Electric field pulses in K and M changes of lightning ground flashes. *Journal of Geophysical Research*, 97(D9), 9935–9950. <https://doi.org/10.1029/92jd00797>
- Rakov, V. A., Uman, M. A., Hoffman, G. R., Masters, M. W., & Brook, M. (1996). Burst of pulses in lightning electromagnetic radiation: Observations and implications for lightning test standards. *IEEE Transactions on Electromagnetic Compatibility*, 38(2), 156–164. <https://doi.org/10.1109/15.494618>
- Saba, M. M. F., Cummins, K. L., Warner, T. A., Krider, E. P., Campos, L. Z. S., Ballarotti, M. G., et al. (2008). Positive leader characteristics from high-speed video observations. *Geophysical Research Letters*, 35(7), L07802. <https://doi.org/10.1029/2007GL033000>
- Scholten, O., Hare, B. M., Dwyer, J., Liu, N., Sterpka, C., Buitink, S., et al. (2021). Time resolved 3D interferometric imaging of a section of a negative leader with LOFAR. *Physical Review D*, 104(6), 063022. <https://doi.org/10.1103/PhysRevD.104.063022>
- Scholten, O., Hare, B. M., Dwyer, J., Liu, N., Sterpka, C., Kolmašová, I., et al. (2021). A distinct negative leader propagation mode. *Scientific Reports*, 11(1), 16256. <https://doi.org/10.1038/s41598-021-95433-5>
- Scholten, O., Hare, B. M., Dwyer, J., Liu, N., Sterpka, C., Kolmašová, I., et al. (2022). Interferometric imaging of intensely radiating negative leaders. *Physical Review D*, 105(6), 062007. <https://doi.org/10.1103/PhysRevD.105.062007>
- Scholten, O., Hare, B. M., Dwyer, J., Sterpka, C., Kolmašová, I., Santolík, O., et al. (2021). The initial stage of cloud lightning imaged in high-resolution. *Journal of Geophysical Research: Atmospheres*, 126(4), e2020JD033126. <https://doi.org/10.1029/2020JD033126>
- Shi, D., Wang, D., Wu, T., & Takagi, N. (2020). A comparison on the E-change pulses occurring in the bi-level polarity-opposite charge regions of the intracloud lightning flashes. *Journal of Geophysical Research: Atmospheres*, 125(17). <https://doi.org/10.1029/2020JD032996>
- Smith, E. M., Marshall, T. C., Karunarathne, S., Siedlecki, R., & Stolzenburg, M. (2018). Initial breakdown pulse parameters in intracloud and cloud-to-ground lightning flashes. *Journal of Geophysical Research: Atmospheres*, 123(4), 2129–2140. <https://doi.org/10.1002/2017JD027729>
- Stolzenburg, M., Marshall, T. C., & Karunarathne, S. (2019). Inception of subsequent stepped leaders in negative cloud-to-ground lightning. *Meteorology and Atmospheric Physics*, 132(4), 489–514. <https://doi.org/10.1007/s00703-019-00702-8>
- Visacro, S., Guimaraes, M., & Murta Vale, M. H. (2017). Features of upward positive leaders initiated from towers in natural cloud-to-ground lightning based on simultaneous high-speed videos, measured currents, and electric fields. *Journal of Geophysical Research: Atmospheres*, 122(23), 12786–12800. <https://doi.org/10.1002/2017JD027016>
- Wang, D., Takagi, N., Uman, M. A., & Jordan, D. M. (2016). Luminosity progression in dart-stepped leader step formation. *Journal of Geophysical Research: Atmospheres*, 121(24), 14612–14620. <https://doi.org/10.1002/2016JD025813>
- Wang, J., Su, R., Wang, J., Wang, F., Cai, L., Zhao, Y., & Huang, Y. (2022). Observation of five types of leaders contained in a negative triggered lightning. *Scientific Reports*, 12(1), 6299. <https://doi.org/10.1038/s41598-022-10366-x>
- Wang, Y., Fan, X., Wang, T., Min, Y., Liu, Y., & Zhao, G. (2021). Characteristics of regular pulse bursts generated from lightning discharges. *Frontiers in Environmental Science*, 9, 799115. <https://doi.org/10.3389/fenvs.2021.799115>
- Wang, Y., Zhang, G., Zhang, T., Li, Y., Zhao, Y., Zhang, T., et al. (2010). The regular pulses bursts in electromagnetic radiation from lightning. In *Asia-Pacific international Symposium on electromagnetic compatibility*, Beijing, China. <https://doi.org/10.1109/APEMC.2010.5475570>
- Yang, J., Wang, D., Huang, H., Wu, T., Takagi, N., & Yamamoto, K. (2023). A 3D interferometer-type lightning mapping array for observation of winter lightning in Japan. *Remote Sensing*, 15(7), 1923. <https://doi.org/10.3390/rs15071923>
- Zhu, B., Zhou, H., Thottappillil, R., & Rakov, V. A. (2014). Simultaneous observations of electric field changes, wideband magnetic field pulses, and VHF emissions associated with K processes in lightning discharges. *Journal of Geophysical Research: Atmospheres*, 119(6), 2699–2710. <https://doi.org/10.1002/2013JD021006>